Supplemental Information for:

Structures of partially occupied hetero-tetramers provide insight into kainate receptor activation and desensitization

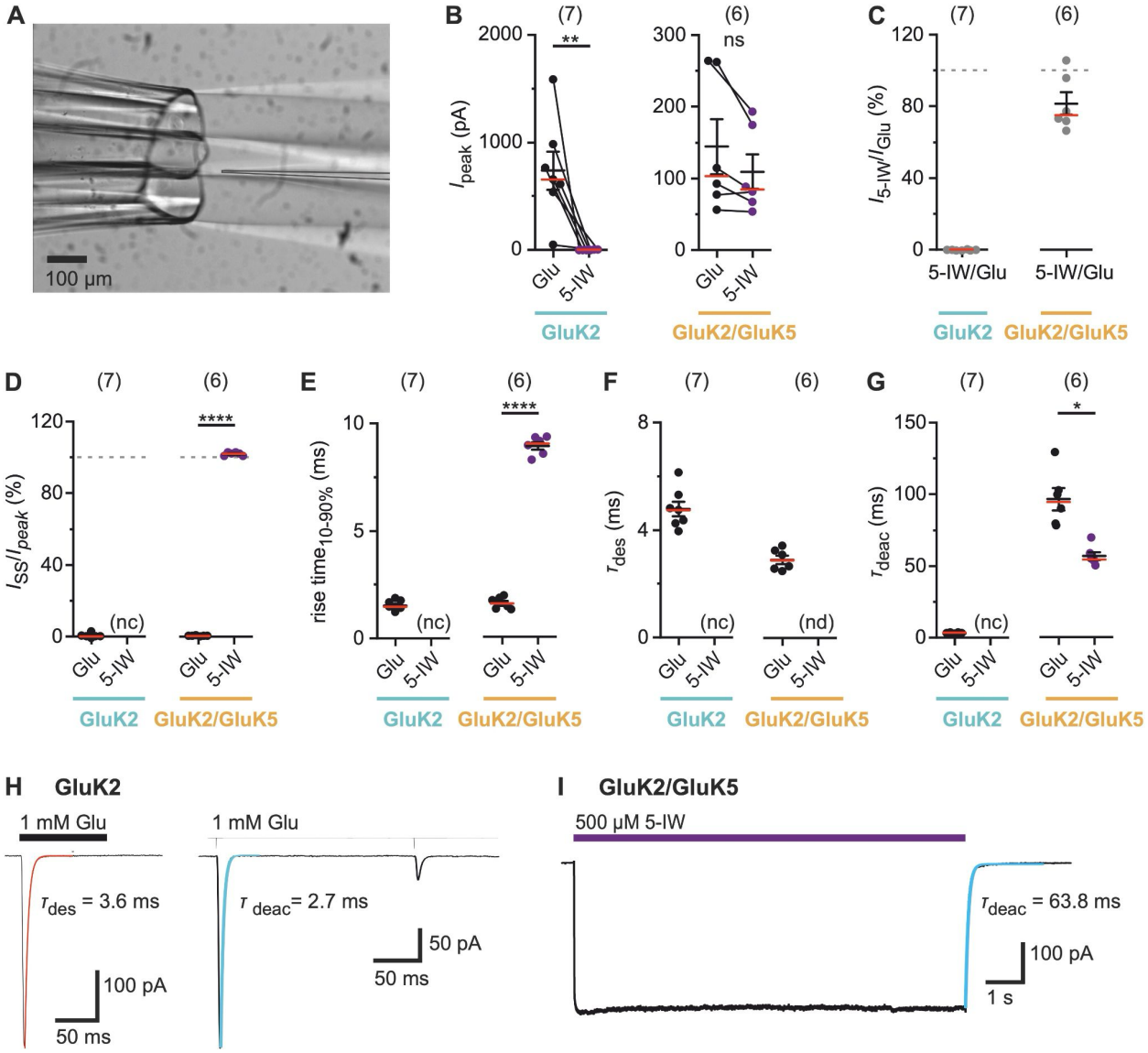
Nandish Khanra*[1,2], Alexa Strauss*[2,3], Laura Moreno Wasielewski*[4], Sophie Lenze[4], Joel Meyerson[1], Andreas Reiner[4#], Joshua Levitz[2,3,5#]

[1] Department of Physiology and Biophysics, Weill Cornell Medicine, New York, NY 10065, USA
[2] Department of Biochemistry and Biophysics, Weill Cornell Medicine, New York, NY 10065, USA
[3] Tri-Institutional Program in Chemical Biology, New York, NY 10065 USA
[4] Faculty of Biology and Biotechnology, Ruhr University Bochum, Bochum, Germany
[5] Department of Psychiatry, Weill Cornell Medicine, New York, NY 10065, USA

* These authors contributed equally

[#] to whom correspondence should be addressed:
andreas.reiner@rub.de or jtl2003@med.cornell.edu

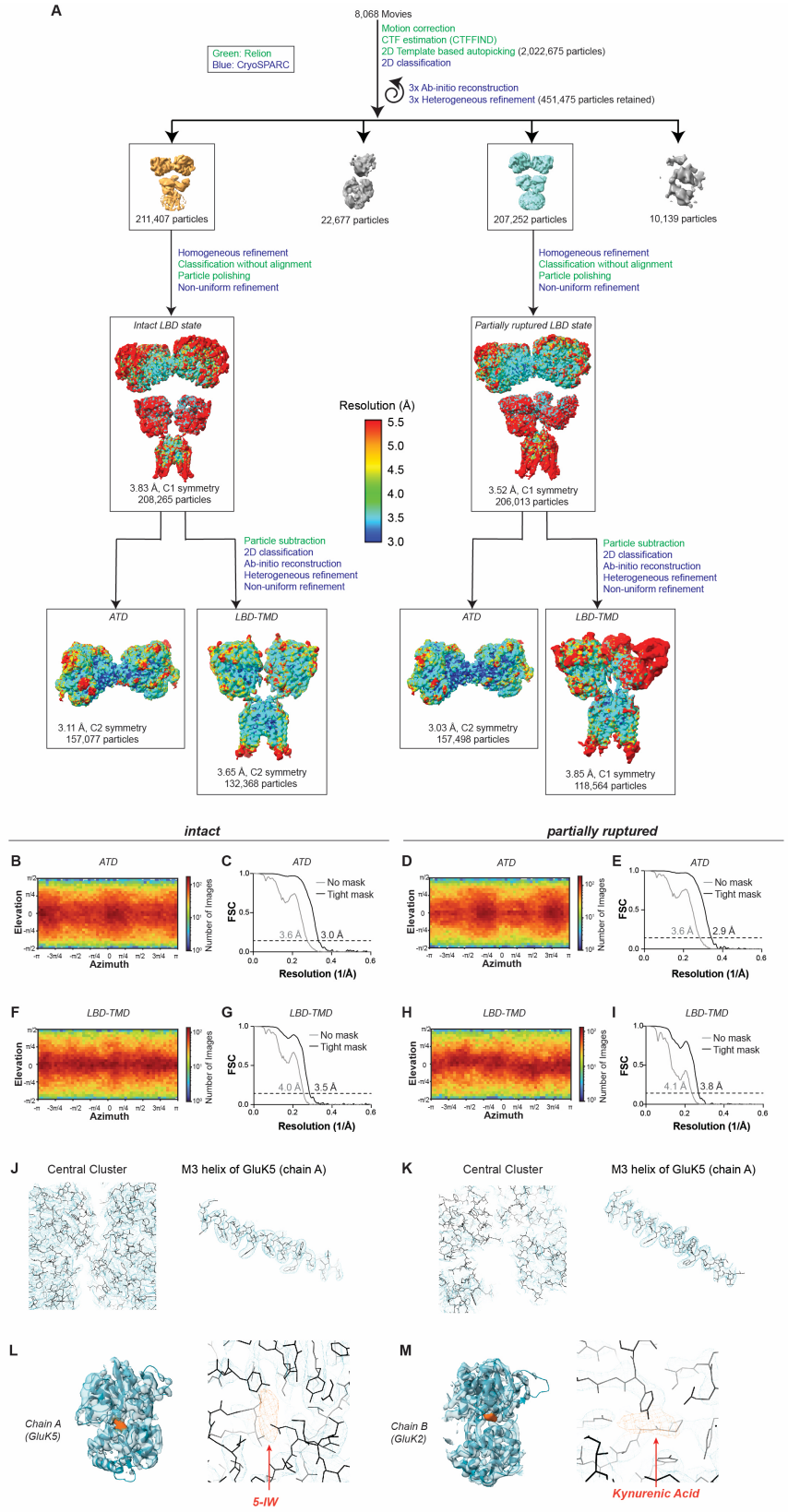
Figure S1, Glutamate and 5-IW responses of GluK2 homotetramers and GluK2/GluK5 heterotetramers



A, Triple-barrel perfusion pipette (left) for applying glutamate and 5-IW to the same cell or membrane patch (patch pipette right, black outline). The central channel contains ligand-free external solution (for visualization, extra salt was added to the outer channels). For example currents see **Fig. 1A**. **B-G,** Data from lifted whole-cells expressing either GluK2 homomers or coexpressing GluK2/GluK5 subunits, obtained with 1 mM glutamate and 500 µM 5-IW. Black lines show means and s.e.m., red lines depict the median (nc, no current; nd, no desensitization; number of measured cells in parentheses). **B,** Peak currents show that 5-IW does not activate GluK2 homomers but GluK2/GluK5 heteromers (paired *t*-tests: ns, not significant; ** $p \leq 0.01$). **C,** Relative current amplitudes. **D,** Steady-state currents of GluK2/GluK5 heteromers show non-desensitizing 5-IW currents (Welch's *t*-test: **** $p \leq 0.0001$). **E,** Comparison of rise times (two-

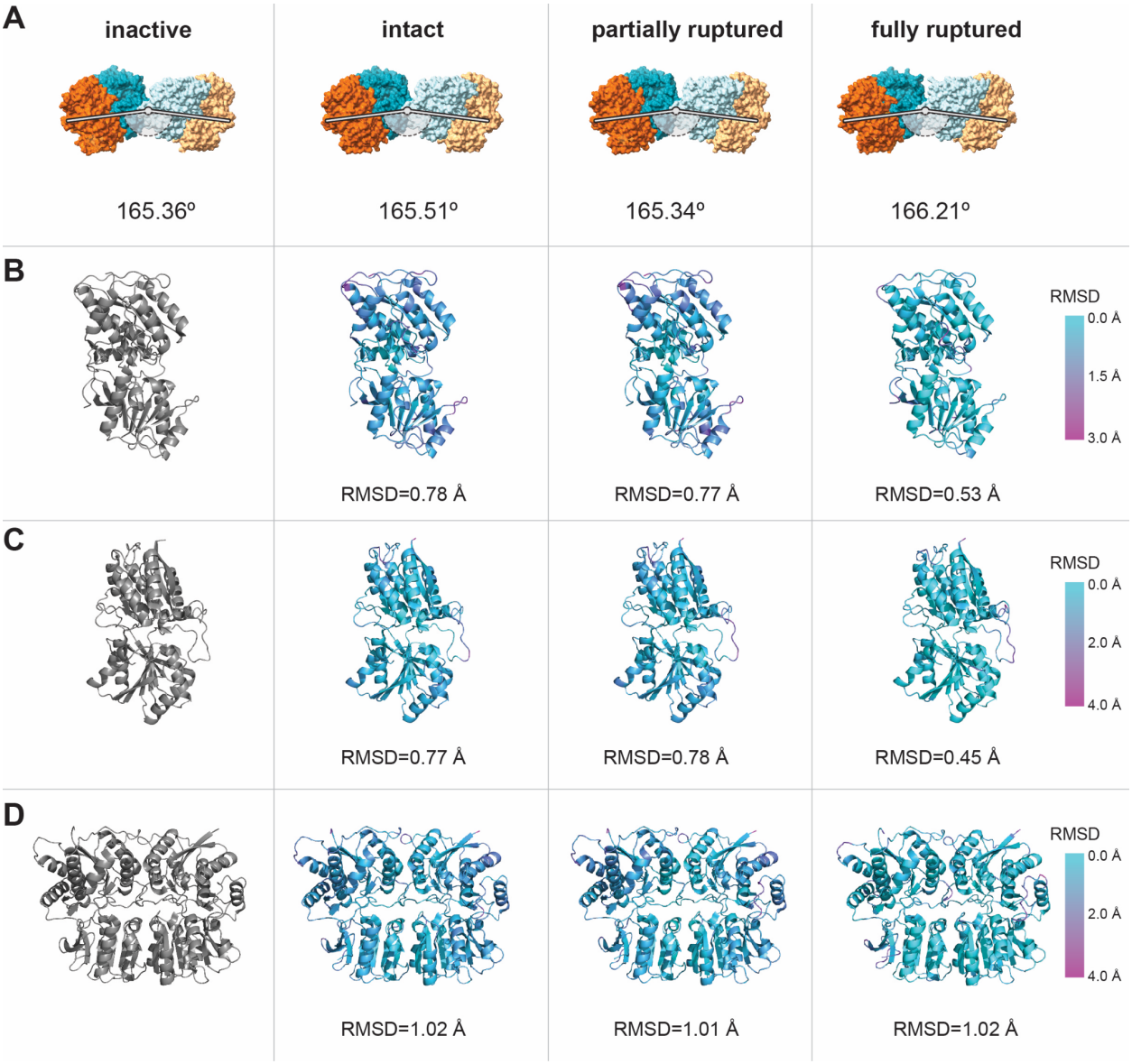
sample *t*-test: **** $p \leq 0.0001$). **F,** Desensitization time constants from single exponential fits. **G,** Deactivation time constants from single or double exponential fits, see **Methods** (Welch's *t*-test: * $p \leq 0.05$). **H**, GluK2 currents in response to long (100 ms) glutamate pulses (left) showing desensitization or two short (0.6 ms) pulses (right) showing deactivation. Desensitization (red line) and deactivation (blue line) were fitted with a single exponential. For quantifications see **Table S2**. For GluK2/GluK5 example currents see **Fig. 4E**. **I,** Extended (10 s) application of 5-IW to a cell containing GluK2/GluK5 heteromers. Deactivation is described by a single exponential (blue line).

Figure S2, Cryo-EM processing pipeline for partially occupied GluK2/K5 heteromer structures



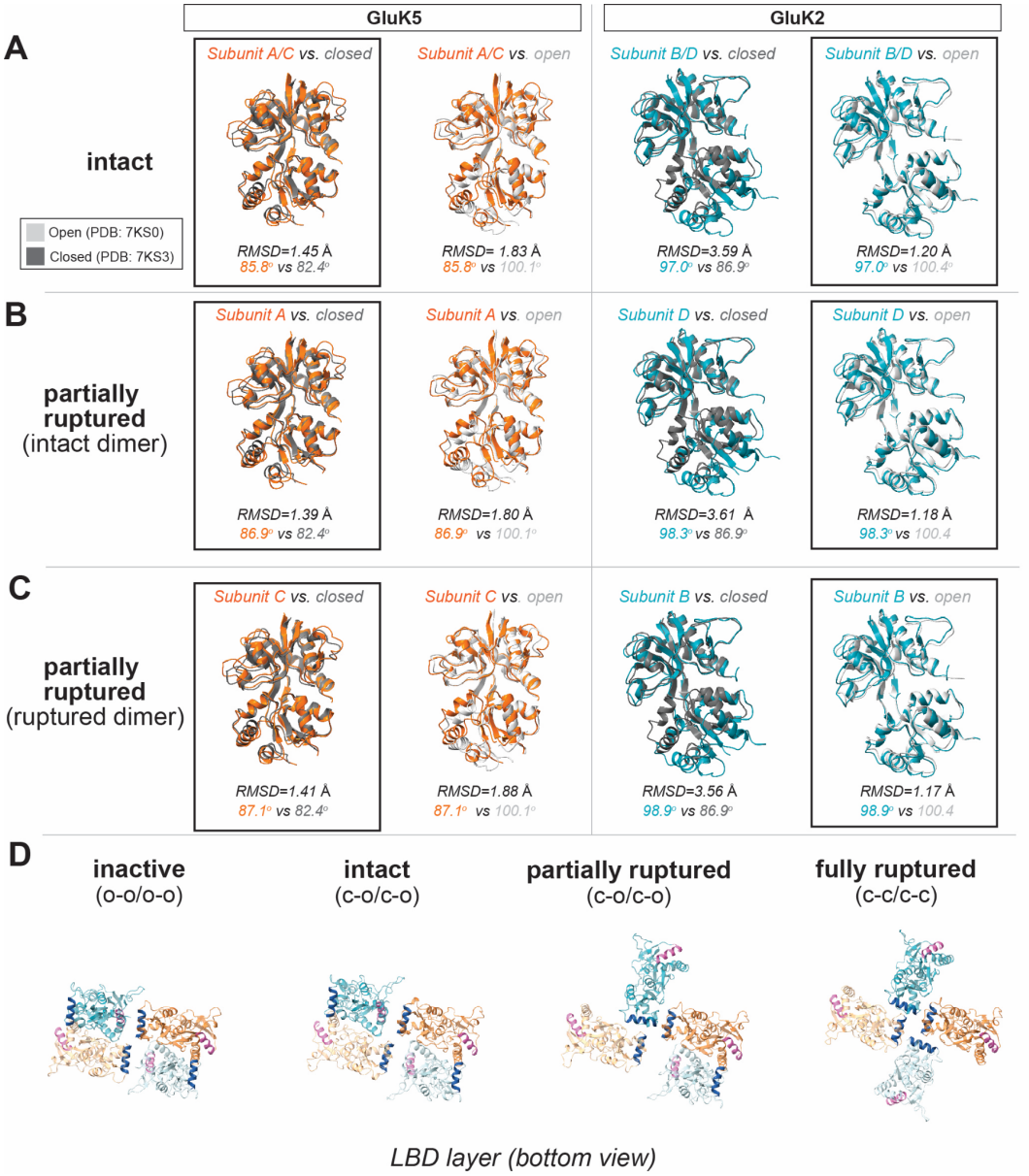
A, Cryo-EM processing pipeline for GluK2/GluK5 treated with 5-IW and kynurenic acid. **B-I,** Angular distribution for particles in the reconstructions produced by cryoSPARC and Fourier shell correlation (FSC) curves for the isolated ATD or LBD-TMD reconstructions. **J-K,** Map/model overlays for key features of the intact (J) and partially ruptured (K) structures. **L-M,** LBD (cyan) and ligand density (orange) for GluK5 (chain A) and GluK2 (chain B) subunits of the intact state.

Figure S3, Analysis of ATD conformations across GluK2/K5 structures



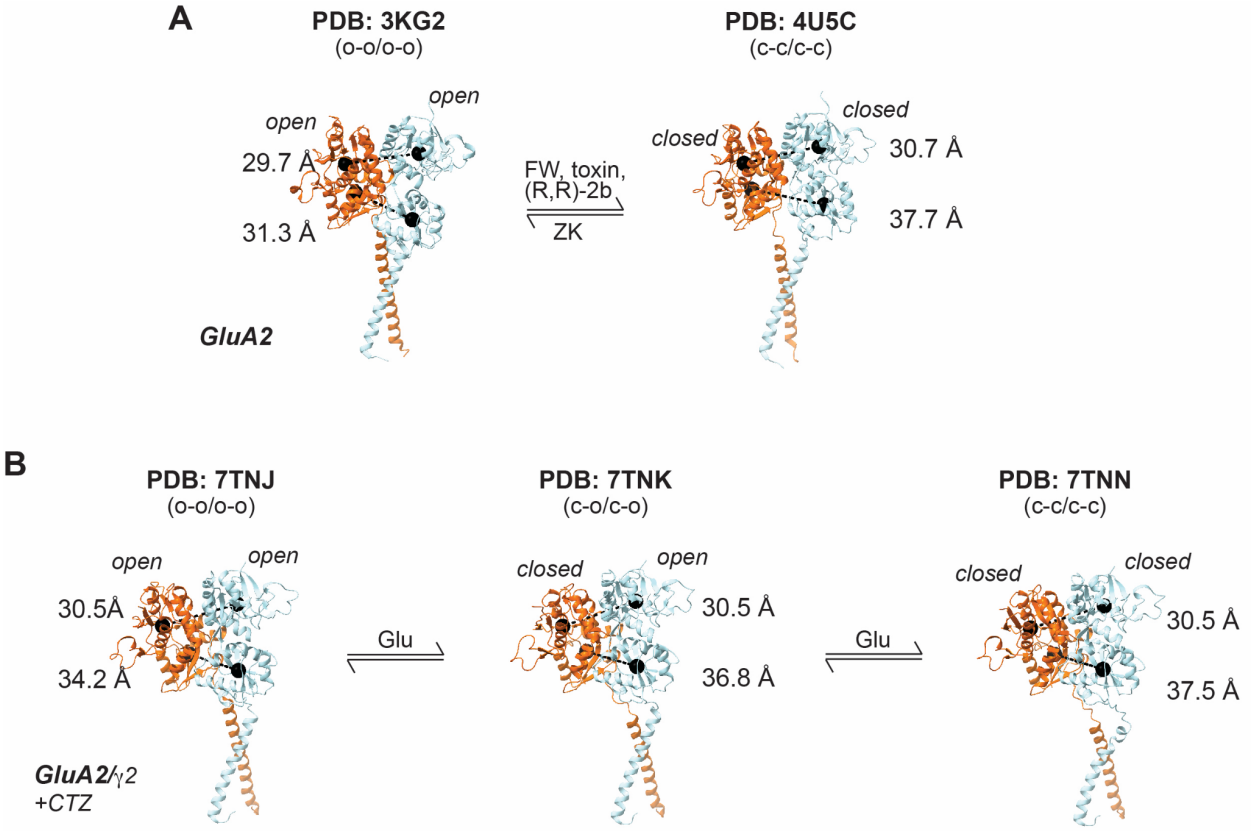
A, Comparison of inter-dimer angle formed by KAR ATD dimer-dimer interface. **B-C,** Comparison of GluK2 (B) and GluK5 (C) ATD monomers aligned to the inactive state. **D,** Comparison of GluK2/GluK5 ATD dimer conformations aligned to the inactive state. ATDs are colored according to RMSD relative to the inactive state. TDs are colored according to RMSD relative to the inactive state.

Figure S4, Further analysis of LBD conformations across GluK2/K5 structures



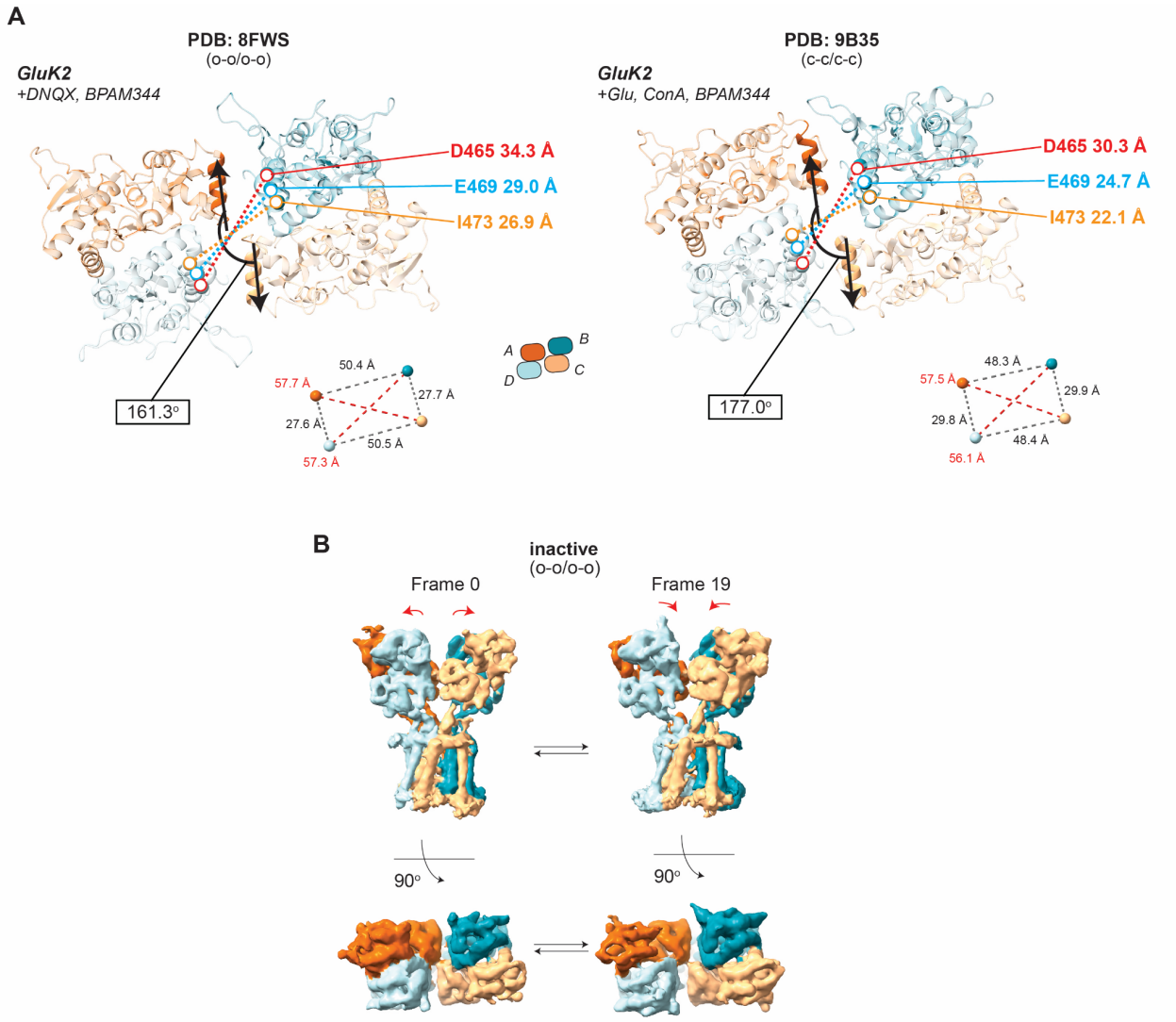
A-C, Analysis of LBD closure (angle between GluK2-F694/T741/A515 or GluK5-F678/T724/A498) and RMSD relative to prior o-o/o-o inactive (PDB 7KS0) and c-c/c-c fully ruptured structures for GluK5 (left) and GluK2 (right) in both intact and partially ruptured structures. **D,** Bottom view of LBD layer across all 4 GluK2/GluK5 structures. Helix G is highlighted in blue and helix B is highlighted in magenta.

Figure S5, Occupancy-dependent LBD dimer rearrangements in AMPARs



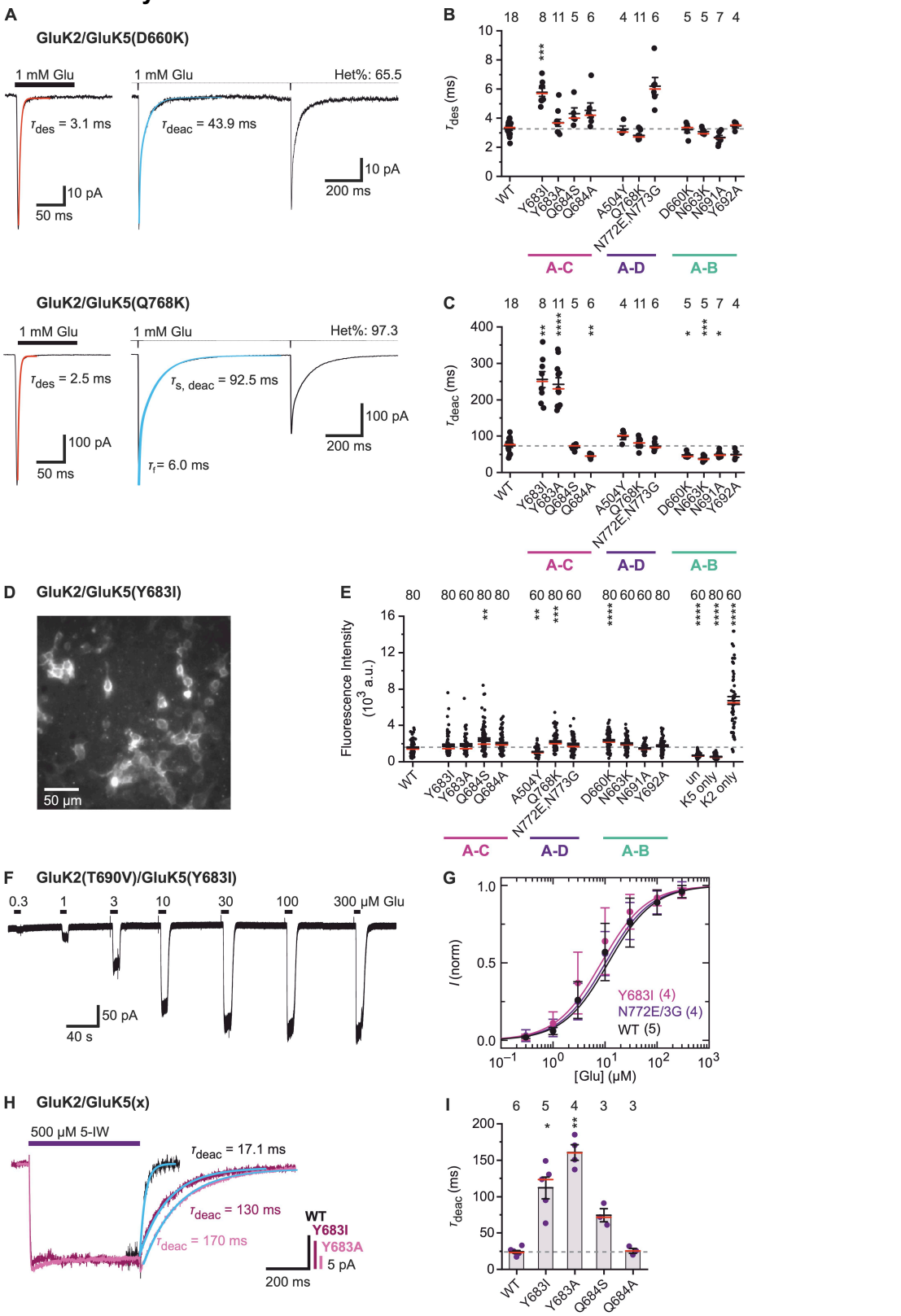
A, Structural comparison between antagonist-bound open/open and partial agonist closed/closed GluA2 LBD homodimers bound to toxin. **B,** Structural comparison between antagonist-bound open/open and glutamate-bound closed/open or closed/closed GluA2 LBD homodimers bound to desensitization blocker CTZ. Note: in these two structures a positive allosteric modulator (BPAM344) was also present. In A and B, center-of-mass distances between upper (D1) and lower (D2) LBD lobes are shown.

Fig S6, Further analysis of inter-dimer LBD conformations across GluK structures



A, LBD layer (top view) of inactive and intact fully occupied GluK2 homo-tetramer structures showing similar intersubunit rotations to those seen for GluK2/GluK5, but with a general decrease in inter-dimer distances (see Fig. 3A). **B,** 3-D variability analysis shows minimal inter-dimer motions in the antagonist-bound state of GluK2/GluK5. Shown are two snapshots from the side (top) and top (bottom) for the major motion component detected.

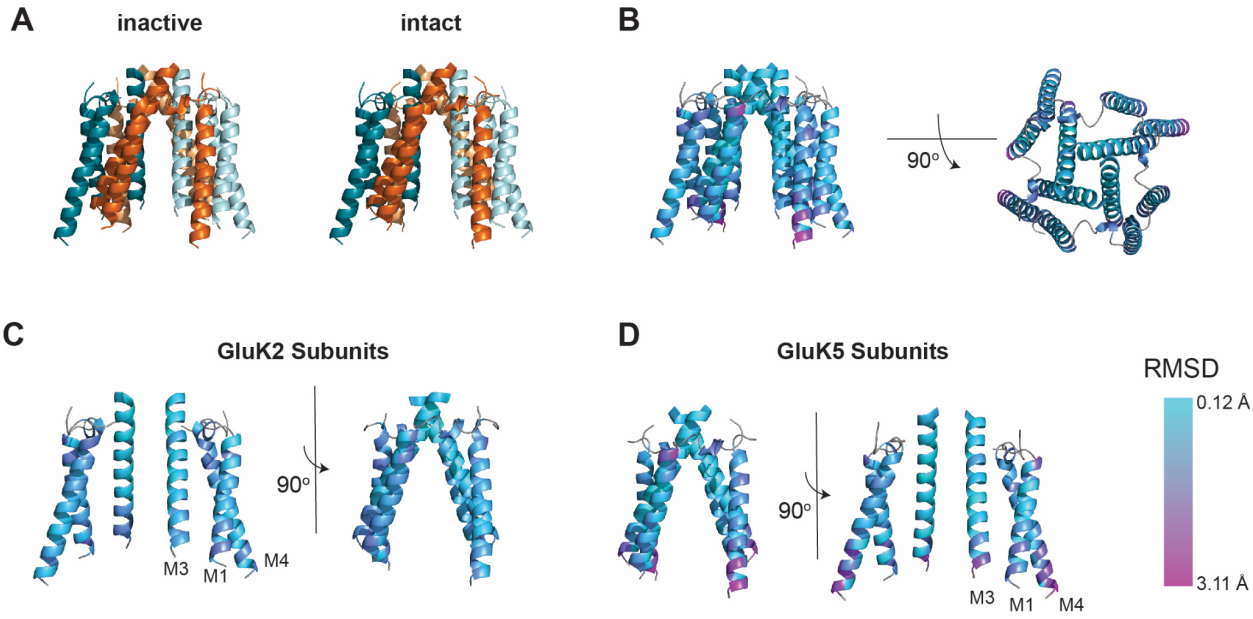
Fig S7, Functional analysis of GluK5 interface variants



A, Example currents of GluK2/GluK5(D660K) and GluK2/GluK5(Q768K) in response to a long (100 ms) glutamate pulses showing desensitization (left) or two short (0.6 ms) pulses showing

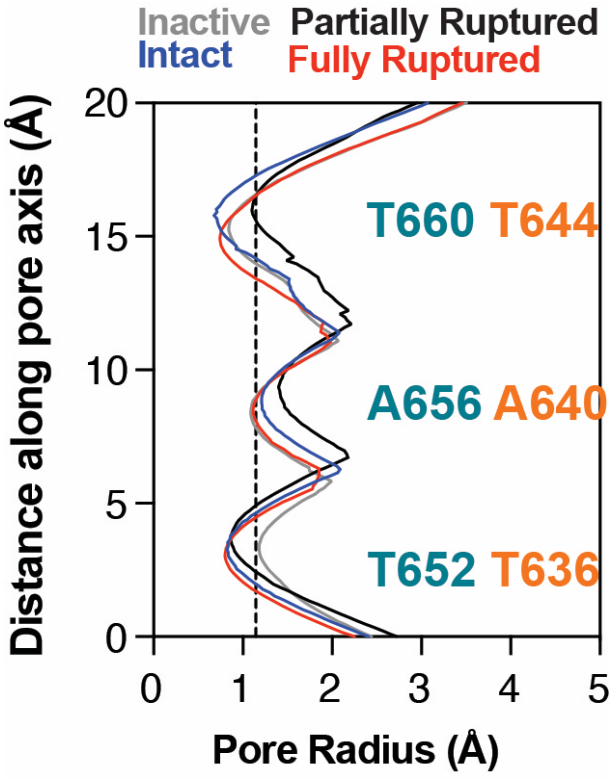
deactivation (right). Desensitization was fitted with a single exponential (red lines) and deactivation experiments with a double exponential function (blue lines). **B,** Summary of glutamate-induced desensitization time constants for all characterized GluK2/GluK5(x) heteromer variants in the A-C, A-D and A-B interfaces (see **Fig. 4**). **C,** Summary of deactivation time constants after short glutamate exposure. For details see **Methods/Analysis.** **D,** Immunocytochemical staining of selected GluK2/HA-SNAP-GluK5(Y683I) heteromers at the cell surface of non-permeabilized HEK cells. An HA-tag antibody (2-2.2.14, Thermo Scientific) was used for staining live cells before fixation and labeling with an AF488-labeled secondary antibody (see **Methods**). **E,** Quantification of fluorescence intensity in the membrane region (see **Analysis**). The mean value of the highest expressing variant (GluK5(Q684S)) is 1.55-fold above wt, the lowest 0.70-fold (GluK5(A504Y)) of wt. Note: HA-SNAP-GluK5 fluorescence is background level (un = untransfected) in the absence of GluK2 co-expression ("K5 only"), whereas HA-SNAP-GluK2 homomer ("K2 only") expression is much higher than any HA-SNAP-GluK5/GluK2 heteromer expression. **F,** Glutamate dose-response measurements for GluK2(T690V)/GluK5(Y683I). The presence of the binding-impaired GluK2(T690V) subunits results in non-desensitizing heteromer currents. **G,** Dose-response curves of GluK2(T690V)/GluK5(wt), GluK2(T690V)/GluK5(Y683I) and GluK2(T690V)/GluK5(N772E,N773G). Averaged normalized currents and s.d. from n= 4-5 cells. Lines show fitted Hill equations (h = 1) with EC_{50} values of 11.52 µM, 8.46 µM and 10.17 µM, respectively (see **Methods/Analysis**). **H,** Example currents of GluK2/GluK5(wt), GluK2/GluK5(Y683I) and GluK2/GluK5(Y683A) in response to 5-IW, measured in outside-out patches. The currents are non-desensitizing (cp. **Fig. 1**). The deactivation kinetics are described by single exponentials (blue lines). **I,** Summary of 5-IW deactivation kinetics for the A-C interface variants. **B-C,E,I** Black lines show means and s.e.m., red lines depict the median. The number of measured lifted-whole cells (B-C), analyzed cell ROIs (E), or outside-out patches (I) is indicated. Statistical testing was performed using a one-way Welch-ANOVA ($p < 0.05$) with a Games-Howell post hoc comparison to wildtype (wt): * $p \leq 0.05$; ** $p \leq 0.01$; *** $p \leq 0.001$; **** $p \leq 0.0001$. For details see also **Table S2**.

Figure S8, Further analysis of TMD conformations between intact GluK2/K5 structures



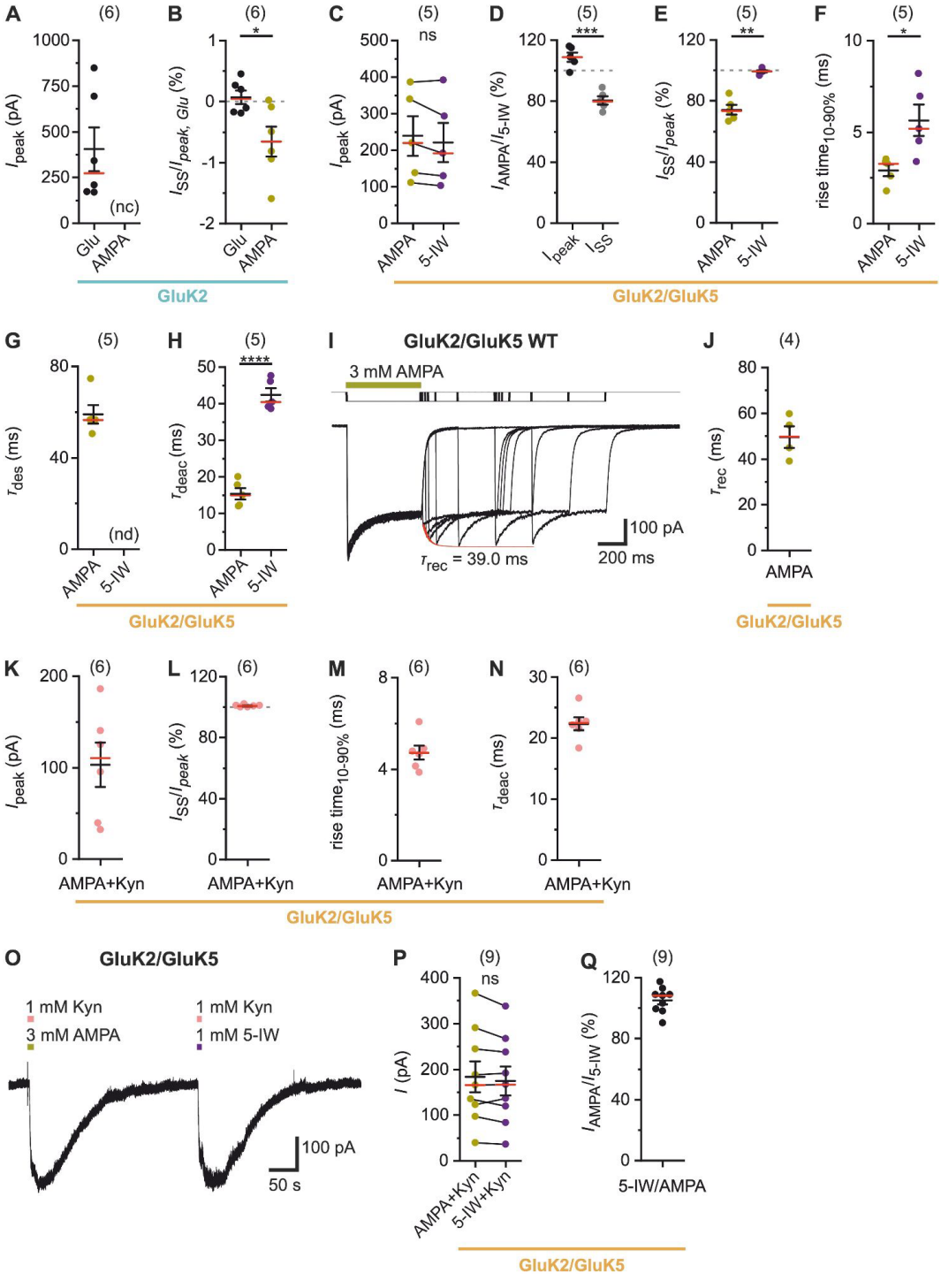
A, Side views of TMD of inactive and intact GluK2/GluK5 structures. **B-D,** RMSD plotted onto the intact structure relative to the inactive structure showing larger changes at the cytoplasmic ends of the helices.

Figure S9, Pore profiles for partially ruptured structure relative to intact and fully ruptured structures



Pore profile showing similar closed states across GluK2/GluK5 structures.

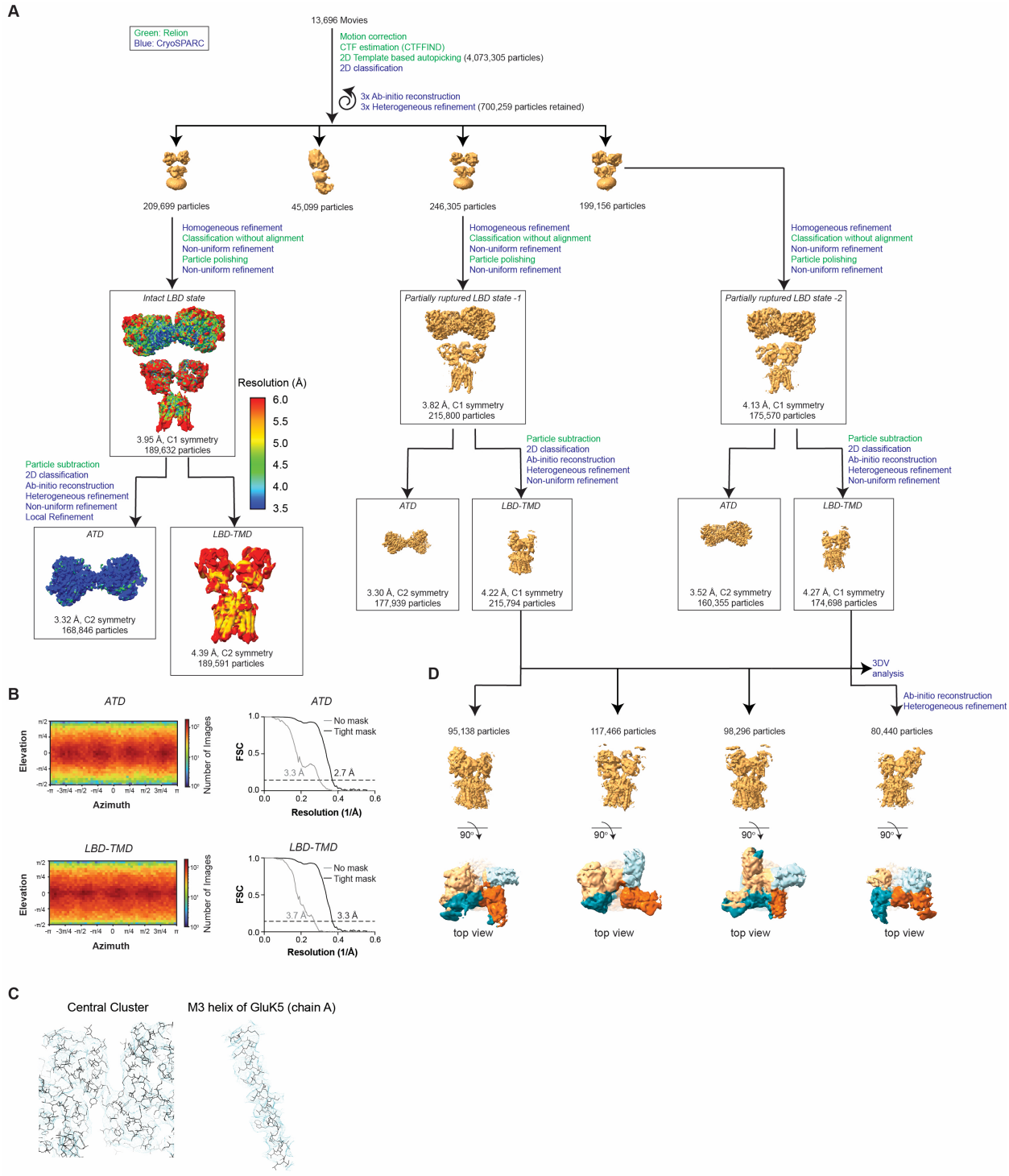
Figure S10, Characterization of GluK2 and GluK2/GluK5 responses to AMPA



A, Data from lifted HEK cells expressing GluK2 homomers show fully desensitizing peak currents in response to 1 mM Glu, but no currents (nc, no current) in response to 3 mM AMPA, see also **Fig. 7A**. **B,** Corresponding steady-state currents normalized to the peak current obtained with glutamate. Negative steady-state currents reflect a minor exchange current. **C-H,** Data from HEK

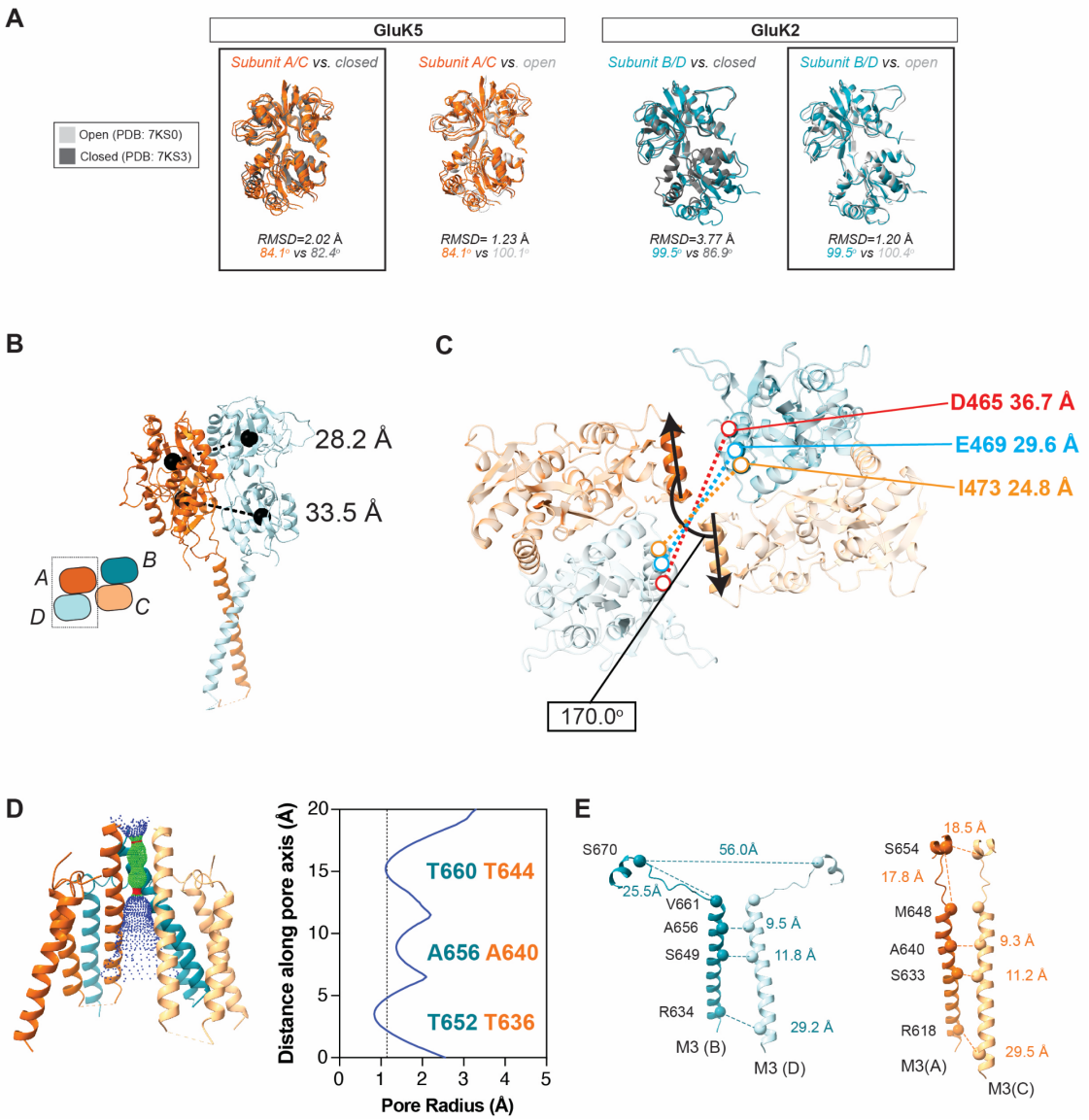
cells coexpressing GluK2/GluK5 subunits (see also **Fig. 7B**). **C,** AMPA (3 mM) and 5-IW (3 mM) induce comparable peak currents. **D**, Comparison of peak and steady currents of AMPA normalized to 5-IW. **E,** Normalized steady-state currents of AMPA show partial desensitization, whereas 5-IW currents are non-desensitizing. **F,** Rise times. **G,** Desensitization time constants of AMPA currents (nd, no desensitization for 5-IW). **H,** Deactivation time constants. **I,** Double-pulse experiment showing fast recovery of GluK2/GluK5 heteromers from AMPA-induced desensitization. The first pulse (green) is followed by a test pulse in variable intervals. **J,** Recovery time constants. **K-N,** Characterization of AMPA-induced currents from GluK2/GluK5 coexpressing cells in the continued presence of 1 mM Kyn, see also **Fig. 7C**. **K**, Peak current amplitudes. **L,** Normalized steady-state currents (~100%) show non-desensitizing AMPA currents. **M,** Rise times. **N,** Deactivation time constants. **O,** Whole-cell recording showing co-applications of AMPA+kynurenic acid and 5-IW+kynurenic acid. Both ligands show similar efficacy. **P,** Current amplitudes. **Q,** AMPA-induced current amplitude normalized to the 5-IW-induced current amplitude. Black lines show means and s.e.m., red lines depict the median. The number of measured cells is shown in parentheses. For statistical testing two-sample *t*-tests were used, except for E where a Welch's *t*-test was used (unequal variance): ns, not significant; * $p \leq 0.05$; ** $p \leq 0.01$; *** $p \leq 0.001$; **** $p \leq 0.0001$.

Figure S11, AMPA processing pipeline



A, Cryo-EM processing pipeline for GluK2/GluK5 treated with AMPA. **B,** Angular distribution for particles in the reconstructions produced by cryoSPARC and Fourier shell correlation (FSC) curves for the isolated ATD or LBD-TMD reconstructions. C, Map/Model overlay for key features of the intact state. **D,** Further processing of the LBD-TMD reconstructions generated from particle subtraction reveals four distinct classes with varying degrees of rupture.

Figure S12, Analysis of intact AMPA-bound GluK2/GluK5 structure



A-D, Structural analysis of LBD closure relative to prior structures (A), LBD dimer arrangements (B), LBD tetramer arrangement (C), pore profile (D), and M3-S2 linker position € for intact AMPA-bound GluK2/GluK5 structure.

Table S1, Cryo-EM statistics of GluK2/GluK5 structures

	GluK2/K5-5IW-Kyn-Intact (full-length)	GluK2/K5-5IW-Kyn-Intact (ATD)	GluK2/K5-5IW-Kyn-Intact (LBD-TMD)	GluK2/K5-5IW-Kyn-Partially ruptured (full-length)	GluK2/K5-5IW-Kyn-Partially ruptured (ATD)	GluK2/K5-5IW-Kyn-Partially ruptured (LBD-TMD)	GluK2/K5-AMPA-Intact (full-length)	GluK2/K5-AMPA-Intact (ATD)	GluK2/K5-AMPA-Intact (LBD-TMD)
Microscope	FEI Titan Krios (NYU)	FEI Titan Krios (NYU)	FEI Titan Krios (NYU)	FEI Titan Krios (NYU)	FEI Titan Krios (NYU)	FEI Titan Krios (NYU)	FEI Titan Krios (NYSBC)	FEI Titan Krios (NYSBC)	FEI Titan Krios (NYSBC)
Camera	Gatan K3	Gatan K3	Gatan K3	Gatan K3	Gatan K3	Gatan K3	Gatan K3	Gatan K3	Gatan K3
Magnification	105,000	105,000	105,000	105,000	105,000	105,000	81,000	81,000	81,000
Voltage (kV)	300	300	300	300	300	300	300	300	300
Electron exposure (e-/Å^2)	49.56	49.56	49.56	49.56	49.56	49.56	51.28	51.28	51.28
Defocus (μm)	1.3-2.0	1.3-2.0	1.3-2.0	1.3-2.0	1.3-2.0	1.3-2.0	1.6	1.6	1.6
Pixel size (Å)	0.826	0.826	0.826	0.826	0.826	0.826	1.083	1.083	1.083
Software	RELION 3.1, cryoSPARC v3.3.2	RELION 3.1, cryoSPARC v3.3.2	RELION 3.1, cryoSPARC v3.3.2	RELION 3.1, cryoSPARC v3.3.2	RELION 3.1, cryoSPARC v3.3.2	RELION 3.1, cryoSPARC v3.3.2	RELION 3.1, cryoSPARC v3.3.2	RELION 3.1, cryoSPARC v3.3.2	RELION 3.1, cryoSPARC v3.3.2
Symmetry imposed	C1	C2	C2	C1	C2	C1	C1	C2	C2
Initial particle images (#)	2,086,593	2,086,593	2,086,593	2,086,593	2,086,593	2,086,593	7,403,033	7,403,033	7,403,033
Final particle images (#)	208,265	157,077	132,368	206,013	157,498	118,564	189,632	168,846	189,591
Map resolution (Å)	3.83	3.11	3.65	3.52	3.03	3.85	3.95	3.32	4.39
FSC threshold	0.143	0.143	0.143	0.143	0.143	0.143	0.143	0.143	0.143
Local map resolution range (Å)	3.0-5.0	2.5-4.5	3.0-5.0	3.0-5.0	2.5-4.0	3.0-5.0	3.5-5.0	3.0-4.5	3.5-5.0

Table S2, Summary of functional data

GluK2	I_{peak} (pA)	$I_{steady\text{-}state}$ (%) [a]	τ_{desen} (ms)	$\tau_{deactivation}$ (ms)	*n*		
WT	737.4 ± 177.7	0.3 ± 0.4	4.8 ± 0.3	3.1 ± 0.1	7		
GluK2/ GluK5(x)	I_{peak} (pA)	$I_{steady\text{-}state}$ (%) [a]	τ_{desen} (ms)	$\tau_{deactivation}$ (ms)	*n*	heteromer content and range (%)	GluK2 position [c]
WT	193.4 ± 58.7	0.4 ± 0.1	3.3 ± 0.1	73.7 ± 4.9	18	65.8 ± 4.9 (26-100)	-
Y683I	216.0 ± 68.5	-1.2 ± 0.4	5.8 ± 0.3	255.5 ± 22.2	8	70.5 ± 5.3 (49-96)	I699
Y683A	336.2 ± 92.0	-0.3 ± 0.3	3.7 ± 0.2	241.9 ± 18.4	9	62.4 ± 6.6 (25-90)	I699
Q684S	265.1 ± 155.4	0.4 ± 0.2	4.3 ± 0.4	65.2 ± 8.9	5	69.2 ± 3.8 (56-77)	S700
Q684A	201.6 ± 78.3	0.6 ± 0.5	4.6 ± 0.5 [b]	45.0 ± 2.3	6	58.2 ± 6.9 (31-78)	S700
A504Y	95.4 ± 45.9	0.4 ± 0.5	3.2 ± 0.2	99.0 ± 8.4	4	42.1 ± 8.0 (28-64)	Y521
Q768K	165.2 ± 48.6	0.4 ± 0.3	2.8 ± 0.1	80.9 ± 4.0	11	74.8 ± 5.6 (41-97)	Q784
N772E,N773G	433.3 ± 88.9	0.4 ± 0.1	6.1 ± 0.6 [b]	72.2 ± 5.7	6	84.3 ± 6.8 (53-100)	E788,G789
D660K	93.6 ± 33.2	0.7 ± 0.2	3.2 ± 0.2	48.0 ± 3.5	5	51.0 ± 5.2 (41-65)	K676
N663K	437.7 ± 27.9	0.0 ± 0.1	3.1 ± 0.1	38.5 ± 3.6	5	44.1 ± 6.7 (35-70)	K679
N691A	159.4 ± 52.8	0.7 ± 0.2	2.7 ± 0.2	49.6 ± 3.4	7	80.3 ± 5.8 (63-100)	A707
Y692A	68.1 ± 29.4	0.5 ± 0.5	3.5 ± 0.2	49.4 ± 7.3	4	69.2 ± 11.3 (37-87)	F708

Currents and kinetic parameters obtained from lifted HEK cells co-expressing GluK2 and different GluK5 variants after exposure to 1 mM glutamate (100 ms pulses for desensitization and 0.6-1 ms double pulses for deactivation; see **Fig. 4** and **Fig. S7** for examples). All values are means with s.e.m. obtained from *n* cells. For details on fitting and heteromer assessment see **Methods**.

[a] None of the variants showed significant steady-state currents; negative values might result from minor exchange currents.

[b] In these variants desensitization was better described by a double exponential fit with a minor slow phase (< 16%). The weighted mean time constant is reported.

[c] Numbering according to rat GluK2, Uniprot seq P42260.

Table S3, Primer Sequences

Substitution	Forward Primer (5'-)	Reverse Primer (5'-)
GluK2(Q621R)	GTTGGCGCCCTCATGAGACAAGGTTCTGAGCTC	GAGCTCAGAACCTTGTCTCATGAGGGCGCCAAC
GluK2(T690V)	GAGGACGGCGCAGTCATGACGTTTTTTAAG	CTTAAAAAACGTCATGACTGCGCCGTCCTC
GluK5(Y683I)	CAGAACTCACGGATCCAGACGTACCAGCG	CGCTGGTACGTCTGGATCCGTGAGTTCTG
GluK5(Y683A)	CTTCTTTCAGAACTCACGGGCCCAGACGTACCAG	CTGGTACGTCTGGGCCCGTGAGTTCTGAAAGAAG
GluK5(Q684S)	CAGAACTCACGGTACTCAACGTACCAGCGGATG	CATCCGCTGGTACGTTGAGTACCGTGAGTTCTG
GluK5(Q684A)	CTTTCAGAACTCACGGTACGCCACGTACCAGC	GCTGGTACGTGGCGTACCGTGAGTTCTGAAAG
GluK5(A504Y)	CTTCACCATCACCTACGAGAGAGAGAAGGTC	GACCTTCTCTCTCTCGTAGGTGATGGTGAAG
GluK5(Q768K)	GATCACGCTGGCCATCCTGAAACTCCAGGAGAACAAC	GTTGTTCTCCTGGAGTTTCAGGATGGCCAGCGTGATC
GluK5 (N772E,N773G)	CCAGGAGGAGGGCAGGCTGGAGATCC	GGATCTCCAGCCTGCCCTCCTCCTGG
GluK5(D660K)	GCAGACGACTTGGCGAAGCAGACCAACATTG	CAATGTTGGTCTGCTTCGCCAAGTCGTCTGC
GluK5(N663K)	GCGGATCAGACCAAGATTGAGTACGGC	GCCGTACTCAATCTTGGTCTGATCCGC
GluK5(N691A)	CAGCGGATGTGGGCCTACATGCAGTCGAAG	CTTCGACTGCATGTAGGCCCACATCCGCTG
GluK5(Y692A)	GCGGATGTGGAATGCTATGCAGTCGAAGCAGC	GCTGCTTCGACTGCATAGCATTCCACATCCGC